Springer

KSME

Journal of Mechanical Science and Technology 28 (11) (2014) 4361~4367
www.springerlink.com/content/1738-494x
DOI 10.1007/s12206-014-1003-8

Design of a novel knee joint for an exoskeleton with good energy efficiency for load-carrying augmentation †

Hyo-gon Kim[1], Sangdeok Park[2] and Changsoo Han[3,*]

[1]*Department of Mechatronics Engineering, Hanyang University, Sangrok-gu, Ansan, 426-910, Korea*
[2]*Korea Institute of Industrial Technology (KITECH), Sangnokgu, Ansan, 426-910, Korea*
[3]*Department of Robot Engineering, Hanyang University, Sangrok-gu, Ansan, 426-910, Korea*

(Manuscript Received January 1, 2014; Revised July 13, 2014; Accepted September 30, 2014)

Abstract

When a linear actuator is used for rotation motion by a knee joint of an exoskeleton, the specifications of the joint range of motion (ROM) and joint torque change according to how the linear actuator are attached. Moreover, while the linear actuator generates a constant amount of force, the joint torque generated by the actuator changes according to the joint angle, which causes the torque contraction. This makes it difficult to meet the required torque and ROM for walk and stand-to-sit and sit-to-stand (STS) motions while carrying a load. To solve these problems we propose a novel knee joint for an exoskeleton with good energy efficiency during walk and STS motions while carrying a load. The mechanism is composed of a four-bar linkage and an elastic element. Based on an analysis of human motion, the design variables of the joint were optimized and the feasibility of the optimized variables was verified through the simulation. The findings from the simulation results suggest that combining a four-bar linkage with a linear actuator allows a large ROM and good torque performance of the knee joint for walk and STS motions. Moreover, the energy efficiency can be improved because the spring mounted parallel to the actuator can store the energy dissipated as negative work and recycle the energy as positive work.

Keywords: Exoskeleton; Four-bar linkage; Elastic element; PEA; Optimization

1. Introduction

Exoskeleton robots have been developed for a variety of applications. These exoskeletons employ actuators which are suitable for such a purpose. BLEEX and HULC, developed by Berkeley Bionics, employ linear hydraulic actuators [1, 2]. Linear hydraulic actuators have simple and lightweight structures, and are easy to mount and maintain. However, when a linear hydraulic actuator is used for rotation motion, the specifications of the joint's range of motion (ROM) and the torque change according to where the linear actuator is attached. An additional problem is that while the linear actuator generates a constant amount of force, the joint torque generated by the actuator changes according to the joint angle, which causes torque contraction. These problems not only make it difficult for the knee joint of the exoskeleton to meet the required torque and ROM for walk and stand-to-sit and sit-to-stand (STS) motions while carrying a load, but also cause the use of a wastefully more powerful motor to avoid the torque contraction.

In the field of wearable robotics, elastic elements are used for reducing the required power and torque of the actuator. Hollander et al. claimed that using a spring in series with an actuator for the ankle can reduce the peak motor power from 250 W to only 77 W [3]. Collins and Kuo developed an energy-recycling artificial foot that reduced the actuator's required power by capturing the collision energy and returning it for the push-off action [4]. In addition, Wang et al. claimed that the motor power and torque could be reduced using series elastic actuation (SEA) and parallel elastic actuation (PEA), respectively, in the exoskeleton [5].

We here propose a novel knee joint of the exoskeleton for load carrying augmentation. The mechanism is composed of a four-bar linkage and an elastic element. The four-bar linkage allows good torque characteristics in a wide ROM. The elastic element not only prevents the torque contraction, but also decreases the required power and torque of the actuator. The combination of both parts yields suitable performance characteristics in the exoskeleton. The rest of this paper is structured as follows. In Sec. 2, we consider the specifications of the knee joint through the analysis of human motion. In Sec. 3, we introduce the proposed knee joint and the kinematic model. In Sec. 4, we describe the optimization process and the simulation results. We then discuss the results and draw our conclusions in Secs. 5 and 6, respectively.

*Corresponding author. Tel.: +82 31 400 5247, Fax.: +82 31 406 6398
E-mail address: cshan@hanyang.ac.kr
† This paper was presented at the ISR-2013, KINTEX, Seoul, Korea, October 24-26, 2013. Recommended by Guest Editor Byung Kyu Kim

Fig. 1. Prototype of the lower extremity exoskeleton used for human motion analysis.

2. Human motion analysis

Assuming that the exoskeleton is anthropomorphic, its joint angles, torques, and power parallel those of a human being. Therefore, an analysis of human motion was conducted to define the design specifications of the exoskeleton's knee joints. Motions performed while not wearing the exoskeleton and while wearing the exoskeleton could differ. Therefore, we built a prototype of the exoskeleton with a working unit to hang the load. We also analyzed walk and STS motions of a subject wearing the prototype with an additional load of 10 kg. Fig. 1 shows a prototype of the lower extremity exoskeleton. The prototype is composed of the following five passive joints in each leg: hip flexion/extension, hip adduction/abduction, hip rotation, knee flexion/extension, and ankle dorsi-flexion/plantar-flexion joints. To facilitate the wearer's motion, the joint's axes pass through the corresponding human joints, except for the hip rotation joint.

Fig. 2 shows the motion capture experiment. One healthy male subject free from the musculoskeletal and neurological injuries participated (height = 178 cm; weight = 80 kg).

The kinematic data and ground reaction force were recorded with a motion capture system (Raptor-E System, Motion Analysis Corporation, USA) and two force plates (Bertec FP4060-10-2000, Bertec Corporation, USA). Each motion was captured three times.

The joint angle, torque, and power were calculated using SIMM (software for interactive musculoskeletal modeling, Motion Analysis Corporation, USA). The calculated joint angle, torque, and power of the knee during walk and STS motions are shown in Fig. 3. The walking cycle was defined as beginning with the heel strike of one foot and ending at the next heel strike of the same foot [6]. This cycle was divided into the stance phase (about 60% of the gait cycle) and the swing phase (about 40% of the gait cycle) during walk motion. The cycle of the STS motion was defined as beginning at the

Fig. 2. Snapshots of motion capture experiment.

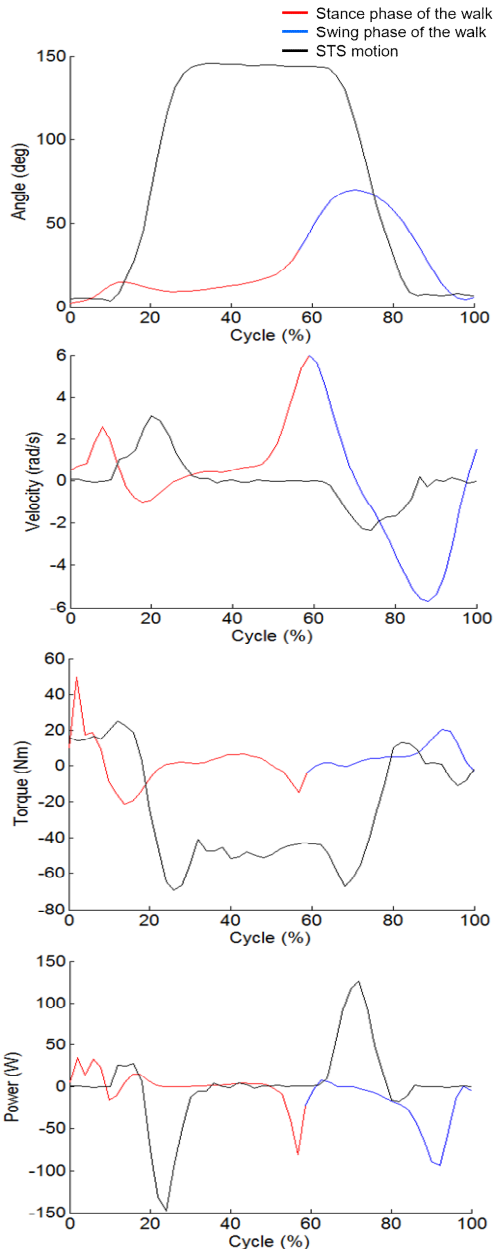

Fig. 3. Captured data of the knee joint during walk and STS motions.

Table 1. Motion capture data of the knee joint.

	ROM (deg)	Velocity (rad/s)	Torque (Nm)	Power (W)
Walk motion	2 ~ 69.8	-5.7 ~ 5.9	-21.2 ~ 49.4	-93.3 ~ 34.4
STS motion	3.4 ~ 145.9	-2.3 ~ 3.1	-67.2 ~ 24.7	-147.4 ~ 125.5
Min. ~Max.	2 ~ 145.9	-5.7 ~ 5.9	-67.2 ~ 49.4	-147.4 ~ 125.5

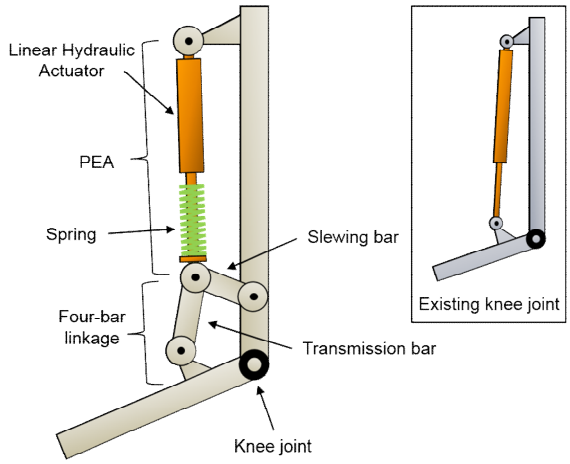

Fig. 4. Simple model of the proposed knee joint.

start of the sitting motion and ending at the end of the standing motion. The power curves show that motion profiles are composed in a complex manner, with the phases of positive and negative power set as positive and negative work, respectively.

The generation of mechanical energy occurs during positive work and the dissipation of mechanical energy occurs during negative work [7]. The elastic element can recycle dissipated energy as negative work when the phase undergoes a transition from negative work to positive work. Table 1 represents the data of the knee's ROM, velocity, torque, and power from minimum to maximum. The knee joints have to meet the requirements set in Table 1. Based on the motion data, the design parameters of the knee joint implemented with the four-bar linkage and elastic elements were optimized.

3. Design of the knee joint

A simple model of the proposed knee joint is shown in Fig. 4. It was designed by combining the PEA and a four-bar linkage. By compressing the spring mounted parallel to the actuator, the spring can store the energy dissipated as negative work and recycle the energy as positive work.

Fig. 5 shows a schematic drawing and the kinematic parameters of the knee joint based on the four-bar linkage. When the linear actuator pushes the slewing bar (L_5), the force is transmitted to the shank-link through the transmission bar (L_6). The force then generates the joint torque. The transmitted force, F_3, and the moment arm change with the angle of the

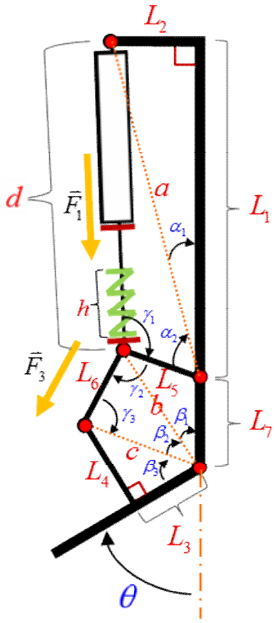

Fig. 5. Schematic drawing and kinematic parameters of the knee joint based on the four-bar linkage.

knee joint. The joint angle (θ) according to the stroke (s) can be derived as follows:

$$\theta = 180 - \beta_1 - \beta_2 - \beta_3 , \tag{1}$$

where

$$\beta_1 = \cos^{-1}\left(\frac{b^2 + L_7^2 - L_5^2}{2bL_7}\right),$$

$$\beta_2 = \cos^{-1}\left(\frac{b^2 + L_3^2 + L_4^2 - L_6^2}{2b\sqrt{L_3^2 + L_4^2}}\right),$$

$$\beta_3 = \tan^{-1}\left(\frac{L_4}{L_3}\right),$$

$$b = \sqrt{L_5^2 + L_7^2 - 2L_5L_7\cos(\pi - \alpha_1 - \alpha_2)},$$

$$\alpha_1 = \tan^{-1}(L_2 / L_1),$$

$$\alpha_2 = \cos^{-1}\left(\frac{L_1^2 + L_2^2 + L_5^2 - d^2}{2aL_5}\right).$$

The joint torque ($\tau_{actuator}$) by the cylinder can be derived as follows:

$$\tau_{actuator} = F_3 \cdot \sqrt{L_3^2 + L_4^2} \cdot \sin\gamma_3 , \tag{2}$$

where

$$F_3 = \frac{F_1 \cdot \sin\gamma_1 \cdot L_5}{\sin\gamma_2 \cdot L_5},$$

$$\gamma_1 = \cos^{-1}\left(\frac{d^2 + L_5^2 - L_1^{\,2} - L_2^{\,2}}{2dL_5}\right),$$
$$\gamma_2 = \pi - \alpha_1 + \alpha_2 - \beta_1 - \beta_2 - \gamma_3,$$
$$\gamma_3 = \cos^{-1}\left(\frac{L_3^{\,2} + L_4^{\,2} + L_6^2 - b^2}{2L_6\sqrt{L_3^{\,2} + L_4^{\,2}}}\right).$$

The joint torque (τ_{spring}) by the spring is

$$\tau_{spring} = \frac{k\Delta h\sqrt{L_3^{\,2} + L_4^{\,2}}\sin\gamma_1 \sin\gamma_3}{\sin\gamma_2}. \quad (3)$$

In this equation, k and Δh denote the stiffness and displacement of the spring, respectively. If Δh is zero, then τ_{spring} is zero. The total torque of the knee joint is derived as follows:

$$\tau = \tau_{actuator} + \tau_{spring}. \quad (4)$$

4. Optimization

4.1 The four-bar linkage

The specifications of the joint's ROM and torque change according to where it is attached and the lengths of the linear actuator, slewing bar, and transmission bar. Therefore, the kinematic parameters of the knee joint must be optimized to meet the requirements shown in Table 2. The design variables are as follows:

$$X = \{L_1, L_2, L_3, L_4, L_5, L_6, L_7\}. \quad (5)$$

Although the linear actuator generates constant force, the joint torque generated changes according to the joint angle, which causes torque contraction, particularly with minimal strokes. However, when the stroke is minimized, the knee angle is the largest; hence, the knee joint has to generate a large amount of torque. Therefore, the following object function has to be maximized:

$$f = \tau(L_1, L_2, L_3, L_4, L_5, L_6, L_7, d, F_1), \quad (6)$$

where

$$d = d_{\min},$$
$$F_1 = A \cdot p.$$

In this equation, p and A denote the pressure in the hydraulic cylinder and the rod's area of the cylinder. In this study, the pressure and the rod's area was set to 54 bar and 1.7671e-04 m^2, respectively. The nonlinear equality constraint for meeting the ROM is

$$C_{eq} = \theta(L_1, L_2, L_3, L_4, L_5, L_6, L_7, d) = 146, \quad (7)$$

Table 2. Optimal design variables.

Design variables	Optimal value (mm)
L_1	319.0
L_2	31.1
L_3	80.8
L_4	-0.8
L_5	88.0
L_6	34.0
L_7	31.0

where

$$d = d_{\min}.$$

The linear inequality constraint for avoiding mechanical interference is

$$AX < b, \quad (8)$$

where

$$A = \begin{bmatrix} 0 & 0 & 1 & 0 & -1 & -1 & 1 \\ -1 & 0 & 0 & 0 & 1 & 0 & 0 \\ 1 & 0 & 0 & 0 & 0 & 0 & 1 \end{bmatrix}$$
$$b = \begin{bmatrix} 0 \\ 0 \\ 350 \end{bmatrix}.$$

Seven design variables have to be optimized. Consequently, the object function should have many local minima. Because a genetic algorithm (GA) does not depend on the starting point, the GA is more likely to find the optimal solution compared with other algorithms using a gradient search depending on the starting point. For these reason, the GA method was used to find optimal design variables that meet the requirements of the ROM and torque.

The optimal design variables are listed in Table 2 and the optimization results are illustrated in Figs. 6 and 7. Fig. 6 represents the ROM of the knee according to the stroke. From this figure, the maximal joint angle is 146° when the stroke is minimum and the maximal stroke is 153 mm. Therefore inequality constraint in Eq. (7) is satisfied.

In Fig. 7, the solid blue line and the solid red line represent the actuator's torque-angle curves created by the optimal four-bar linkage and by the existing mechanism, respectively. Note that the existing mechanism is optimized by the same object function and constraints of four-bar linkage to directly compare with the results of four-bar linkage. In case of the four-bar linkage, the torque meets our requirement in most ROM. In particular, when the joint angle is maximized, the actuator's torque is about 42.04 Nm. Compared to the case of four-bar

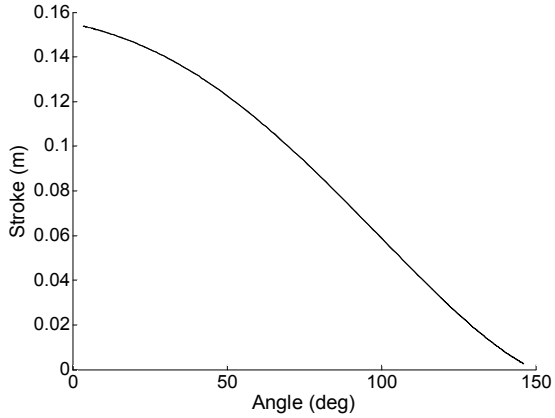

Fig. 6. Stroke-angle curve according to the optimal four-bar mechanism.

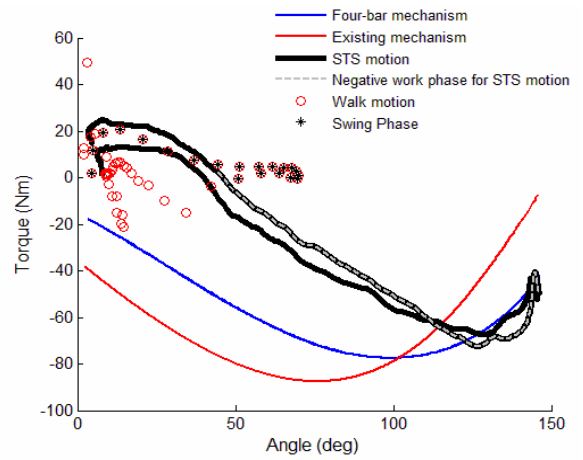

Fig. 7. Torque-angle curve according to the optimal four-bar mechanism.

linkage, the existing mechanism, used in the knee joint of HULC and BLEEX devices, reveals different results. The optimized existing mechanism also meets the requirement of ROM. However, the torque at the joint angle above 114° is significantly decreased. Furthermore, the joint torque at the maximum joint angle drops to about 6.9 Nm. As a result, the torque characteristic of the four-bar linkage is more suitable than the existing mechanism for the walk and STS motions.

4.2 The elastic element

Despite optimization of the four-bar linkage, the problem of torque contraction at large joint angle still remains. Because of the problem, the exoskeleton could not assist the wearer's locomotion required large joint angle (e.g., semi-squat position). To solve the problem, we apply an elastic element to the four-bar mechanism. The operation principle is illustrated in Fig. 8. The spring mounted parallel to the actuator is compressed and stores the energy during stand-to-sit motion. The stored energy is released during sit-to-stand motion. This principle is effective in not only assisting the wearer's locomotion but also reducing the required torque and power of the actuator.

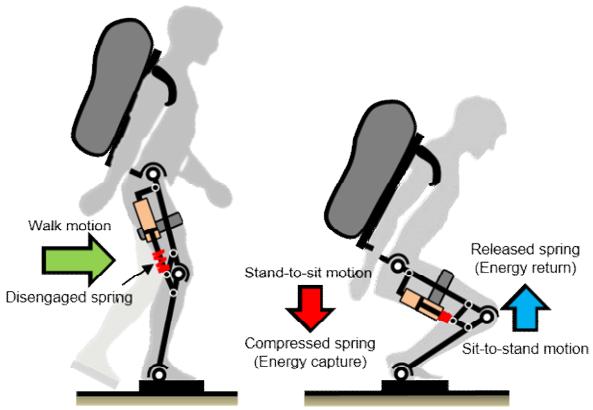

Fig. 8. Operation examples of the elastic element.

To realize these functions, the elastic element was optimized. The design variables are the spring stiffness k and the spring free length h. The object function is as follows:

$$f = \sum_{i=1}^{n} [\tau_i - \tau_{spring,i}]^2 , \quad (9)$$

where τ_i and $\tau_{spring,i}$ denote the joint torque and the spring torque, respectively, at the i-th time instant in the human motion data. If the spring torque is greater than the human torque during negative work, the robot resists the wearer's motion. Thus, we defined the inequality constraint as follows:

$$\tau_i \geq \tau_{spring,i} . \quad (10)$$

We also used an elastic element above 90° at the knee joint to facilitate the wearer's motions such as swinging the leg and stair climbing without resistance. This represents a nonlinear inequality constraint. To optimize the spring parameter, we used *fmincon* function in the MATLAB (Mathworks Inc., Natick, MA), which is based on the interior-reflective Newton method and the sequential quadratic programming method. It was set up to obtain the minimum of the constrained nonlinear multivariable objective function.

The optimal spring stiffness and optimum spring-free length were 12.578 N/mm and 112 mm, respectively. Fig. 9 shows the torque-angle curve in the knee using the optimal variables of the elastic elements. The solid blue line represents the torque-angle curves created by the optimal spring for the knee joint. Because the optimal spring torque is smaller than the human torque during negative work, the spring torque does not resist the wearer's motion.

The spring torque with the maximal angle is 38.65 Nm. In Fig. 10, we illustrate the torque and power generated by the optimal spring (solid blue line) and required torque and power of the actuator (solid red line) as a function of the cycle of STS motions. This result suggests that the required torque and

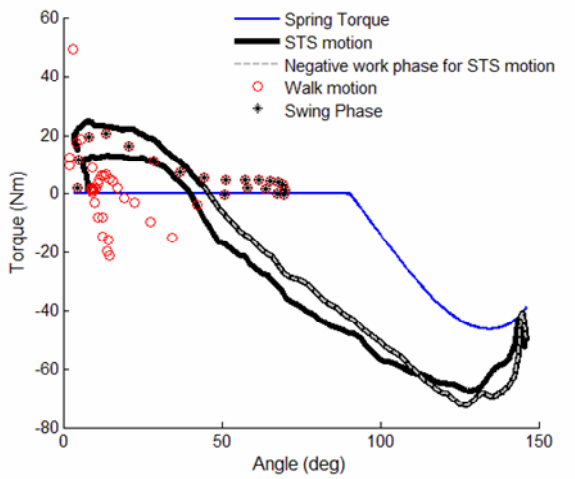

Fig. 9. The torque-angle curve according to the optimal spring.

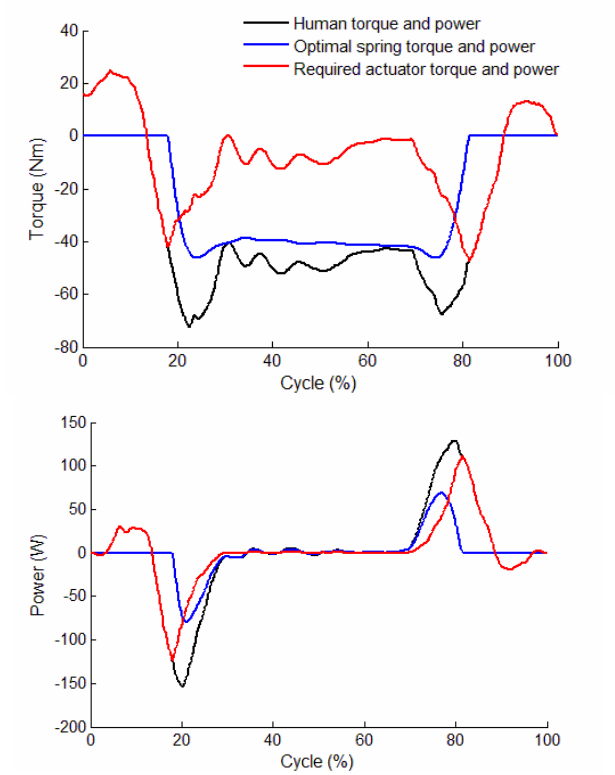

Fig. 10. The torque and power by the optimal knee spring.

power of the actuator are significantly decreased because the actuator has only to generate the residual power, with exception of the spring power. Ideally, energy saving rate by the optimized spring, which is calculated by Eq. (11), is 34.5 %.

$$\left[\frac{\sum|Total\ human\ power| - \sum|\mathrm{Re}sidual\ power|}{\sum|Total\ human\ power|}\right]\times 100\% . \tag{11}$$

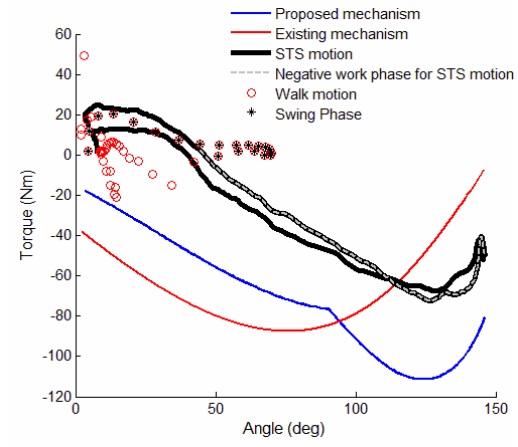

Fig. 11. The torque-angle curves by the proposed mechanism.

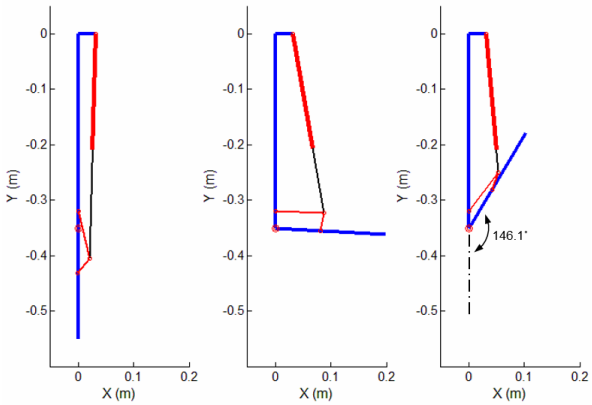

Fig. 12. Graphical simulation results of proposed knee joint.

5. Discussion

On the basis of the optimization results, we performed a simulation in MATLAB to verify the feasibility of the results. Fig. 11 shows that proposed novel knee joint can generate much more torque than required torque in whole ROM. Furthermore, as described in Sec. 4.2, the sufficient torque margin by the optimal spring could contribute to high energy efficiency of the exoskeleton. The graphical results of the proposed knee joint are illustrated in Fig. 12. The results show that all constraints we define are satisfied: ROM is 146.1˚, a space for installing the compressed spring is 40 mm, and there is no mechanical interference. So, the optimized design variables are feasible. Therefore, we expect that the proposed mechanism can support the wearer well as compared to existing mechanisms during walk and STS motions.

To apply the proposed mechanism to a hydraulically powered exoskeleton, the specifications of the motor, pump, and cylinder have to be determined. To do this, the plots of flow rate according to the cycle and joint angle are used (see Fig. 13). Assuming that the displacement of the pump and the diameter of the rod in the actuator are 0.51 cc/rev and 0.015 m, respectively, the maximal speed of motor is then 6829 rpm during the transition from the stance phase to the swing phase.

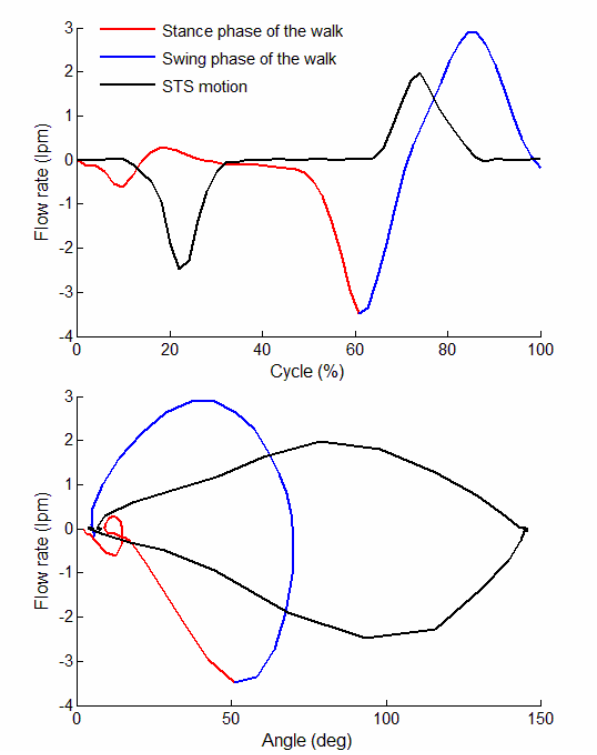

Fig. 13. Required flow rate according to the proposed mechanism.

6. Conclusions

We have proposed a novel knee joint for an exoskeleton. The mechanism is composed of a four bar linkage and an elastic element. The design variables, associated with the actuator placement and spring specifications, are optimized and the feasibility of the variables is verified through the simulation. The simulation results suggest that combining a four-bar linkage with a linear actuator allows a large ROM and good torque performance of the knee joint for walk and STS motions. Moreover, the energy efficiency can be improved because the spring mounted parallel to the actuator can store the energy dissipated as negative work and recycle the energy as positive work.

As future work, we are implementing the proposed mechanism into a real exoskeleton and are experimentally investigating its effects.

Acknowledgment

This work was supported by the Duel-Use Technology Program of MOTIE/DAPA/CMTC. [13-DU-MC-16, High speed lower-limb exoskeleton robot control at rough terrain]

References

[1] A. B. Zoss, H. Kazerooni and A. Chu, Biomechanical design of the Berkeley lower extremity exoskeleton (BLEEX), *Mechatronics, IEEE/ASME Transactions on*, 11 (2) (2006) 128-138.

[2] K. N. Gregorczyk, L. Hasselquist, J. M. Schiffman, C. K. Bensel, J. P. Obusek and D. J. Gutekunst, Effects of a lower-body exoskeleton device on metabolic cost and gait biomechanics during load carriage, *Ergonomics*, 53 (10) (2010) 1263-1275.

[3] K. W. Hollander, R. Ilg, T. G. Sugar and D. Herring, An efficient robotic tendon for gait assistance, *Journal of Biomechanical Engineering*, 128 (5) (2006) 788-791.

[4] S. H. Collins and A. D. Kuo, Recycling energy to restore impaired ankle function during human walking, *PLoS one*, 5 (2) (2010) e9307.

[5] S. Wang, W. van Dijk and H. van der Kooij, Spring uses in exoskeleton actuation design, *In Rehabilitation Robotics (ICORR), IEEE international Conference on* (2011) 1-6.

[6] V. T. Inman, H. J. Ralston and F. Todd, *Human walking*, Williams & Wilkins (1981).

[7] P. DeVita, J. Helseth and T. Hortobagyi, Muscles do more positive than negative work in human locomotion, *Journal of Experimental Biology*, 210 (19) (2007) 3361-3373.

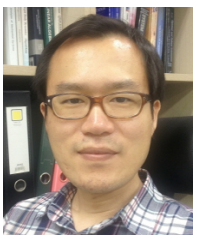

Hyo-gon Kim received the B.S. degree with 2nd major in control and instrumentation engineering and M.S. degree in Mechanical Design & Manufacturing Engineering from Changwon National University, Korea, in 2005 and 2008, respectively. He is currently a Ph.D. candidate at the Department of Mechatronics Engineering in Hanyang University, and also a research assistant in the Robotics R&BD Group at the Korea Institute of Industrial Technology (KITECH). His research interests include compliance control for hydraulic robots, design and control for exoskeleton systems.

Sangdeok Park received his B.S. degree in Mechanical Design at Yeungnam University in 1998 and M.S. and Ph.D. degrees from the department of Mechanical Engineering at Pohang University of Science and Technology (POSTECH) in 1990 and 2000, respectively. He is a principal researcher with a chief officer of Robotics R&BD group of KITECH. His research interests include the design and control of quadruped walking robots, wearable robots and hydraulically driven robots.

Changsoo Han received the Ph.D. in Mechanical Engineering from the University of Texas at Austin, USA, in 1989. He is a Professor of Robotics in the Department of Robot Engineering, Hanyang University, South Korea. His research interests include exoskeleton systems, biomechanical rehabilitation systems and automation in construction.